Single-Shot Time-Resolved Measurements of Nanosecond-Scale Spin-Transfer Induced Switching: Stochastic Versus Deterministic Aspects

T. Devolder,[1] J. Hayakawa,[2,3] K. Ito,[2] H. Takahashi,[2] S. Ikeda,[3] P. Crozat,[1] N. Zerounian,[1] Joo-Von Kim,[1] C. Chappert,[1] and H. Ohno[3]

[1]*Institut d'Electronique Fondamentale, CNRS UMR 8622, Bât. 220, université Paris-Sud, 91405 Orsay, France*
[2]*Hitachi, Ltd., Advanced Research Laboratory, 1-280 Higashi-koigakubo, Kokubunji-shi, Tokyo 185-8601, Japan*
[3]*Laboratory for Nanoelectronics and Spintronics, Research Institute of Electrical Communication, Tohoku University, 2-1-1 Katahira, Aoba-ku, Sendai 980-8577, Japan*

(Received 25 June 2007; revised manuscript received 16 October 2007; published 7 February 2008)

Using high bandwidth resistance measurements, we study the single-shot response of tunnel junctions subjected to spin torque pulses. After the pulse onset, the switching proceeds by a ns-scale incubation delay during which the resistance is quiet, followed by a 400 ps transition terminated by a large ringing that is damped progressively. While the incubation delay fluctuates significantly, the resistance traces are reproducible once this delay is passed. After switching, the time-resolved resistance traces indicate micromagnetic configurations that are rather spatially coherent.

DOI: 10.1103/PhysRevLett.100.057206 PACS numbers: 75.60.Ej

The spin-transfer effect [1,2] is one of the most investigated phenomena in the recent advances of magnetism. It results from the exchange of angular momentum between a spin current and a nanomagnet [3], inducing torques that can be used to manipulate magnetic configurations. This leads to new phenomena such as the displacement of domain walls [4], the generation of magnons [5], and steady magnetization orbits [6,7]. The spin torque (ST) can also simply switch the magnetization of a nanomagnet [8] for instance in a magnetic tunnel junction (MTJ). This is considered as promising for information storage, since this type of switching has proven scalability, speed and energy efficiency [9].

However, in ST experiments the entanglement between magnetization-dependent transport properties and current-dependent magnetization dynamics makes the understanding of the dynamics a formidable task. In metallic spin-valves, the understanding is even rendered more complex by the symmetry breaking induced by the Ampere-field inherently associated with the transport of electrons. To that respect, the MTJ are simpler, because the needed current for switching (hence the Ampere field) is much smaller [10].

Partial understanding of the switching has already been obtained by using stroboscopic techniques to follow the ensemble-averaged magnetization response [11–14]. These methods have succeeded in determining the mean switching path and speed. However, the switching is known not to be deterministic [6,15] at room temperature [16,17], but any variance of the switching was suppressed with the previously used techniques [11–14] because of their stroboscopic natures.

In the present Letter, we report the first single-shot time-resolved measurements of ns-scale ST switching events. We separate the reproducible features in the switching behavior from the features that fluctuate. We show that the stochasticity of the switching does not result from a chaotic magnetization trajectory but only from a fluctuation of an incubation delay.

Our results were checked on six devices patterned from a MTJ of composition CoFeB (2.5)/MgO (0.9)/CoFeB (6)/Ru(0.8)/CoFe(5)/MnIr(8), with thicknesses in nm. The switchable magnet is the $Co_{40}Fe_{40}B_{20}$ (2.5) free layer. The bottom electrode CoFeB (6) has its magnetization

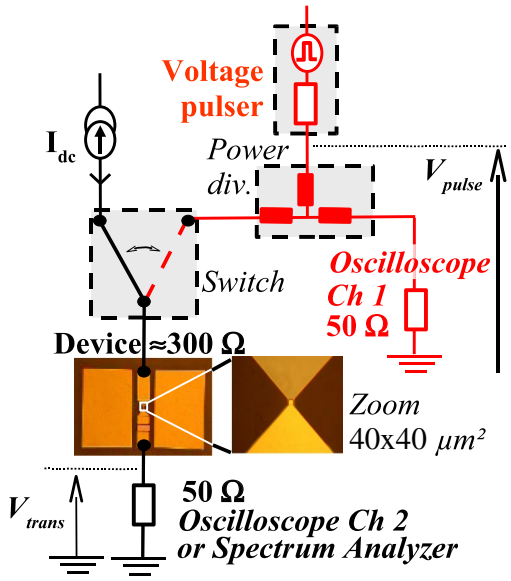

FIG. 1 (color online). Experimental setup. A switch allows to exchange the low and high frequency configurations. The optical micrographs are the high frequency coplanar circuit (500 × 500 μm^2) and a zoom (40 × 40 μm^2) of its central part around the MTJ. The square shaped overlap of top and bottom triangular electrodes is 3 μm wide. The MTJ is buried below.

fixed by antiferromagnetic coupling with the CoFe layer which is exchange biased. The MTJ is patterned in a 100×300 nm^2 rectangle. The long axis is along the pinning direction. The MTJ is sandwiched between coplanar leads in a high bandwidth circuit (Fig. 1).

The static properties are gathered in Fig. 2; panel A displays 60 loops measured with 10 μA at 20 loops/s. The tunnel magnetoresistance ratios were between 30 and 50% with resistance-area products of 11 $\Omega \cdot \mu$m^2. The loops show back and forth abrupt transitions between high (AP, antiparallel) and (P, parallel) low resistance states. The loops are off-centered, indicating that the free layer senses a 2.8 mT coupling with the bottom electrode. This coupling favors the P state, and previous studies indicated that it is a dipolar interaction with the uncompensated synthetic antiferromagnet. The reversible slope in the AP branch indicates that the magnetization is not saturated in that branch: the sizable dipolar coupling distorts the AP state near the tips of the free layer. Conversely, the remanent P state seems saturated. Figure 2(c) gathers 60 ST loops, measured at 1 kloops/s. The mean AP to P switching voltage was 0.6 V, while the mean P to AP switching voltage was -0.7 V, both a variance of ± 0.1 V. MTJ breakdown occurs at 1.2 V.

Our Stoner astroids [Fig. 2(b)] are compiled from easy axis loops, each of them being measured for a constant hard axis field. Each loop provides two astroid points, taken as the fields of extremal loop slope. In addition to the easy axis coupling, the astroids are also systematically slightly off-centered along the hard axis by -0.7 mT. The origin of this coupling is unclear, but is compensated in the results described below. Not compensating it resulted in slightly faster switching but similar conclusions.

The loop shape is consistent with the uniaxial anisotropy expected from the device shape. However, the anisotropy cannot be extracted from the corners of the room temperature astroid. Indeed for hard axis applied fields, apparent saturation of the magnetization (i.e., $\langle R(t) \rangle \approx R_P + 0.5\Delta R$ where $\langle\rangle$ denotes quasistatic measurement) is reached 2–3 mT away from the astroid center. We stress that this saturation is only apparent: $R(t)$ undergoes in fact telegraph noise between two levels $R_{\text{low}} \approx R_P + 0.2\Delta R$ and $R_{\text{high}} = R_P + 0.8\Delta R$ [Fig. 2(d)]. Hard axis fields greater than 8 mT were required to make R_{high} and R_{low} states converge to a unique state with constant resistance $R(t) \approx R_P + 0.5\Delta R$. The anisotropy field is thus 8 mT.

To examine the eigenexcitations of our system, we have measured their voltage noise [18]. We applied small currents (30 μA) to avoid generating ST-induced oscillations [7], but high fields to get uniformly magnetized states. Two modes were detectable as peaks in the spectra [Fig. 3(a)] at frequencies f_{low} and f_{high}. For both modes, the $(2\pi f/\gamma)^2$ curves increase linearly with field. Assuming a Landé factor of 2.1 and the corresponding gyromagnetic ratio γ, the respective slopes are 0.44 ± 0.01 T and 0.66 ± 0.05 T. Considering our noise level, a linear extrapolation to $f^2 = 0$ is reasonable only for f_{low}. The intersection happens at -7 ± 4 mT. Since this value recalls the free layer anisotropy, and knowing that the effective magnetization M_{eff} of CoFeB alloys is much thickness dependent [19], we attribute f_{low} to the free layer, that thus have $\mu_0 M_{\text{eff}} = 0.44$ T. The higher frequency and less intense mode is likely to arise from excitations in the pinned layer.

For convenience, we translate resonance linewidth Δf into effective damping parameters, using: $\Delta f \approx \alpha_{\text{EFF}} \gamma_0 (M_{\text{eff}} + 2H + 2H_k)$ which [19] is valid when $f_{\text{FMR}} \gg \Delta f$ for a macrospin. This yields $\alpha_{\text{EFF}} = 0.006 \pm 0.001$ for the free layer, close to Gilbert damping [19]. The pinned CoFeB(5) layer has a much broader linewidth (2 GHz) that is likely to be dominated by extrinsic contributions, as often observed [20] in layers submitted to large exchange coupling.

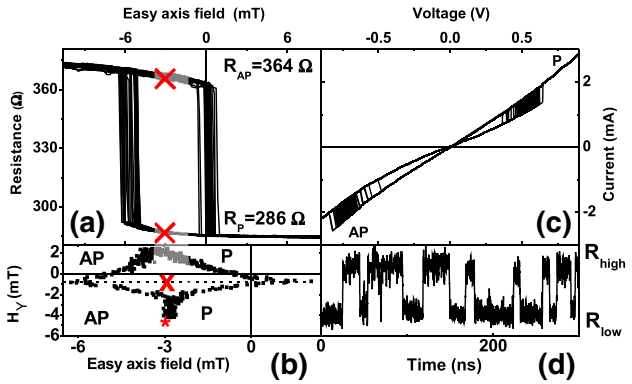

FIG. 2 (color online). (a) Superimposition of 60 easy axis hysteresis loops. The cross symbols define the two remanent positions (b) Stoner astroid measurement. (c) Current versus voltage traces for applied field parameters taken at the center of the astroid. (d) time-resolved resistance of a device when subjected to a hard axis field of -5 mT, i.e., at the position of the + symbol of panel (b).

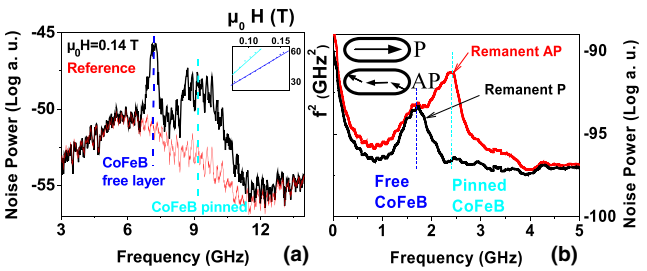

FIG. 3 (color online). (a) Power Spectra of the voltage noise emitted by a device when submitted to 140 mT and 0 V (red reference curve) or 0.1 V (black curve). Inset: zoom on a part of the field dependence of the square of the peak frequencies. (b) Power Spectra of the voltage noise in the two remanent states at the astroid center. The small ripple in the spectra is an artifact. Inset: sketch of the proposed micromagnetic configurations at remanence.

It is also interesting to examine the noise spectra at remanence [Fig. 3(b)]. Free layer excitations at 1.6 GHz are detected at both remanences. In contrast, the peak of the pinned layer at 2.9 GHz is detected only in the AP state. This is a further support to the existence of unsaturated magnetization at the tips of free layer at the AP remanence. Indeed some non collinearity of the magnetizations of the free and pinned layers is required [18] to render our setup linearly sensitive to the small fluctuations of very stable the pinned layer.

Let us now investigate ST switching in its fastest limit, i.e., for applied voltages just below breakdown. We restrict our analysis to the P to AP switching, since the remanent P state seems saturated which ensures a well defined initial state.

The measurement is done as follows: a proper field sequence sets the sample in the P state. A (negative) voltage step V_{pulse} is then applied with a rise time of 55 ps. A power divider routes half of the pulse to the device. The transmitted voltage V_{trans} is recorded with a single-shot 13 GHz oscilloscope (Fig. 1). With this setup, the voltage drop across the MTJ is very near V_{pulse}. V_{trans} scales with the current and decreases abruptly at the switching instant [inset of Fig. 4(a)]. Following the analytical methodology of [21], the temperature rise during the pulse can be estimated to be at most 10 K. The steady temperature is reached instantly, since due to the high thermal conductivities (circa 100 $\mathrm{W/m \cdot K}$) of all layers, a steady thermal flow from the pillar to the electrodes is established in less than 10 ps. Additional constant current experiments (not shown) confirm that the magnetization intensity is not affected by the current, hence that the heating is very limited.

In Fig. 4, we display 20 responses $V_{\text{trans}}(t)$ to voltage steps of -1 V. The switching instants are distributed between 0 and at least 10 ns, with a mean value of 5.3 ns. Boosting the voltage to -1.1 V reduces the mean switching duration to 2.5 ns. To better evidence the oscillations in $V_{\text{trans}}(t)$, we have calculated resistance traces. For this, we assume that whenever the switching failed, the device resistance had stayed constant in time. So we use the average $V_{\text{trans}}(t)$ on unsuccessful trials to deduce $V_{\text{pulse}}(t)$ [22], and then $R(t)$ of any trial.

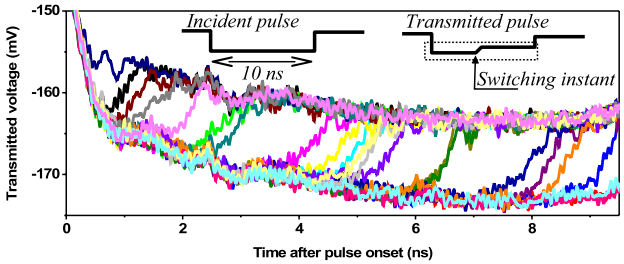

FIG. 4 (color online). Inset: sketch of the incident and transmitted voltage pulses when a device switches from P to AP. Main panel: zoom on the plateau of the transmitted voltage pulse for a -1 V incident voltage step: each of the 20 events is displayed in a different color.

The three top traces in Fig. 5(a) are resistance records of single-shot events. Among single-shot traces, we selected two events (no. 1 and no. 2) with equal switching instants of 1.65 ns. The noisy traces in Fig. 5(a) correspond to those two events measured with 13 GHz bandwidth. The topmost curve is another record of event no. 1, after mathematical 3 GHz low pass filtering. There is an incubation delay before anything detectable happens after the pulse onset. It is followed by a rounded departure from R_p to $R_p + 0.2\Delta R$ [Fig. 5(b)]. Then, the transition from $R_P + 0.2\Delta R$ to R_{AP}-$0.2\Delta R$ is abrupt and takes 0.4 ns. Finally, there is a pronounced ringing. To study this ringing, we have constructed lower noise traces while keeping the full bandwidth. For this, we choose a given switching instant (here 1.65 ns) and average the full bandwidth traces corresponding to events that have that specific switching instant, to get the bottom curve in Fig. 5(a). While it does not reveal additional facts, it confirms that the ringing is reproducible with a frequency of 1.4 ± 0.2 GHz and a decay time of 1.5 ± 0.5 ns.

We have repeated the averaging procedure for selected switching instants of 0.7 to 4.9 ns [Fig. 5(b)]. It is striking to see that the $R(t)$ curves only differ by their incubation delay: the subsequent resistive signature of the switching trajectory (ringing amplitude, frequency, and damping rate) is reproducible.

The modeling of our findings would require extensive simulations which are beyond the scope of this paper. Instead, we discuss some possible switching scenarios. The absence of any electrical signature before the switching indicates that the reversal is not triggered by the

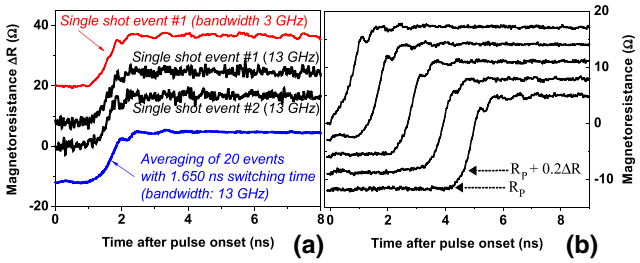

FIG. 5 (color online). Panel (a) top curve: Single-shot switching event measured with 3 GHz bandwidth. Second curve: same single-shot switching event measured with 13 GHz bandwidth. Third curve: another single-shot switching event, manually selected because it has the same switching instant, measured with 13 GHz bandwidth. Bottom curve; average of 20 single-shot switching events measured with 13 GHz bandwidth, those events having the same switching instant. Panel (B) average of single-shot switching events measured with 13 GHz bandwidth, those events having the same switching instant. From top to bottom curves, the switching instants are 0.7, 1.6, 2.8, 3.9, and 4.9 ns. The curves are vertically offset for clarity.

pumping of the FMR mode like in a macrospin-type reversal [23]. Also, the switching does not seem to be driven by the amplification and beating of two mirror-symmetric C-bended states as would be favored by the Ampere field. This scenario would indeed lead to features that are not observed, e.g., an oscillation of $R(t)$ before the switching and a quiet $R(t)$ after (see Fig. 2 in [24]). It is also unlikely that the ST excites a spin wave mode with an odd number of nodal lines, for which the local precessions could give resistance variations that cancel each other perfectly: such modes have frequencies that are significantly above the lowest mode in our kind of samples [25].

The slow regular change from R_p to $R_p + 0.2\Delta R$ after the incubation delay rather argues in favor of an inhomogeneous response, with only tips or corners of the free layer reacting before the main transition. This inhomogeneous character interplays with the fact that any local tilting of the magnetization alters the local conductivity and dynamically redistributes the current inside the sample. A tip of the nanomagnet may react first, until its magnetization is sufficiently tilted to propagate the disturbance to the nanomagnet center, triggering then the fast reversal. Since the details of the initial micromagnetic configurations are thermally distributed, the switching duration fluctuates from pulse to pulse, like in any nucleation phenomenon.

At the switching instant the system can be viewed as undergoing a strong percussional excitation. Among the sample eigenmodes, there is, in particular, the quasiuniform precession mode, whose frequency recalls that of the ringing. In the absence of ST, this mode would decay with a characteristic time of ${t_{\mathrm{decay}}}^0 \approx 2/(\alpha_{\mathrm{EFF}}\gamma_0(M_S + 2H_k)) \approx 4.3$ ns. In the AP state after switching, the negative current provides an additional source of damping approximately equal to the natural damping [11] such that the lifetime is reduced by half to 2.1 ns. This expected decay rate is in fair agreement with the measured decay time of the ringing, indicating a high coherence of the sample's behavior after switching.

In summary, we have investigated the switching induced by pulsed spin torques on rectangular MTJs. The reversal occurs after a random ns-scale incubation delay. During that delay, there is no measurable signature of some large magnetization precession inside a fraction of the sample. Once initiated, the switching itself proceeds in a transition lasting reproducibly 0.4 ns, and is always followed by a pronounced oscillation of the electrical resistance. The frequency and decay rate of this ringing indicate a high spatial coherence after switching, recalling the macrospin image.

[1] J. Slonczewski, J. Magn. Magn. Mater. **159**, L1 (1996).
[2] L. Berger, Phys. Rev. B **54**, 9353 (1996).
[3] M. D. Stiles and A. Zangwill, Phys. Rev. B **66**, 014407 (2002).
[4] M. Yamanouchi, D. Chiba, F. Matsukura, and H. Ohno, Nature (London) **428**, 539 (2004).
[5] B. Özyilmaz, A. D. Kent, J. Z. Sun, M. J. Rooks, and R. H. Koch, Phys. Rev. Lett. **93**, 176604 (2004).
[6] A. V. Nazarov, H. Seok Cho, J. Nowak, S. Stokes, and N. Tabat, Appl. Phys. Lett. **81**, 4559 (2002).
[7] S. I. Kiselev, J. C. Sankey, I. N. Krivorotov, N. C. Emley, R. J. Schoelkopf, R. A. Buhrman, and D. C. Ralph, Nature (London) **425**, 380 (2003).
[8] J. A. Katine, F. J. Albert, and R. A. Buhrman, Appl. Phys. Lett. **77**, 3809 (2000).
[9] T. Devolder, A. Tulapurkar, Y. Suzuki, C. Chappert, P. Crozat, and K. Yagami, J. Appl. Phys. **98**, 053904 (2005).
[10] J. Hayakawa, S. Ikeda, Y. M. Lee, R. Sasaki, T. Meguro, F. Matsukura, and H. Takahashi, Jpn. J. Appl. Phys. **44**, L1267 (2005).
[11] I. N. Krivorotov, N. C. Emley, J. C. Sankey, S. I. Kiselev, D. C. Ralph, and R. A. Buhrman, Science **307**, 228 (2005).
[12] R. H. Koch, J. A. Katine, and J. Z. Sun, Phys. Rev. Lett. **92**, 088302 (2004).
[13] N. C. Emley, I. N. Krivorotov, O. Ozatay, A. G. F. Garcia, J. C. Sankey, D. C. Ralph, and R. A. Buhrman, Phys. Rev. Lett. **96**, 247204 (2006).
[14] Y. Acremann, J. P. Strachan, V. Chembrolu, S. D. Andrews, T. Tyliszczak, J. A. Katine, M. J. Carey, B. M. Clemens, H. C. Siegmann, and J. Stohr, Phys. Rev. Lett. **96**, 217202 (2006).
[15] T. Devolder, C. Chappert, J. A. Katine, M. J. Carey, and K. Ito, Phys. Rev. B **75**, 064402 (2007).
[16] M. L. Schneider, M. P. Pufall, W. H. Rippard, S. E. Russek, and J. A. Katine, Appl. Phys. Lett. **90**, 092504 (2007).
[17] T. Devolder, C. Chappert, and K. Ito, Phys. Rev. B. **75**, 224430 (2007).
[18] S. E. Russek, R. D. McMichael, M. J. Donahue: in *Spin Dynamics in Confined Magnetic Structures*, edited by B. Hillebrands and K. Ounadjela (Springer, Berlin, Heidelberg, 2003), Vol. II.
[19] C. Bilzer, T. Devolder, J. V. Kim, G. Counil, C. Chappert, S. Cardoso, and P. P. Freitas, J. Appl. Phys. **100**, 053903 (2006).
[20] B. Heinrich, in *Ultrathin Magnetic Structures, Vol. III*, edited by J. A. C. Bland and B. Heinrich (Springer-Verlag, Berlin, 2005).
[21] R. C. Sousa, M. Kerekes, I. L. Prejbeanu, O. Redon, B. Dieny, and J. P. Nozieres, J. Appl. Phys. **95**, 6783 (2004).
[22] This estimate agrees with the data of channel 1 of the oscilloscope. However, the constructed $V_{\mathrm{pulse}}(t)$ cannot simply be replaced by that data, because of frequency dependent losses and delays in the circuitry that distort the rising phase of the pulse and cannot be corrected.
[23] J. Z. Sun, Phys. Rev. B **62**, 570 (2000).
[24] K. Ito, T. Devolder, C. Chappert, M. J. Carey, and J. A. Katine, J. Phys. D **40**, 1261 (2007).
[25] McMichael and Stiles, J. Appl. Phys. **97**, 10J901 (2005).